Electronic Structure of Layered Oxides Containing M_2O_7 (M = V, Nb) Double Octahedral Slabs

Roger Rousseau,[1a] Maria Rosa Palacín, Pedro Gómez-Romero,* and Enric Canadell*,[1b]

Institut de Ciència de Materials de Barcelona (CSIC), Campus de la UAB, 08193 Bellaterra, Spain

Received August 9, 1995[⊗]

The electronic structure of M_2O_7 double octahedral slabs with low d electron counts has been studied. It is shown that the nature of the low d-block bands is strongly dependent on the d electron count and the distortions of the layer. All d^1 systems are expected to be similar and to exhibit Fermi surfaces which result from the superposition of both one-dimensional (1D) and two-dimensional (2D) contributions. For lower d electron counts the electronic structure is quite sensitive to the existence of M−O bond alternations perpendicular to the layer and off-plane distortions of the equatorial O atoms. The Fermi surface of these systems can either be purely 2D or have 1D and 2D portions like those of the d^1 systems. It is suggested that the recently reported phase $Rb_2LaNb_2O_7$ could be a 2D metal. It is also proposed that chemical reduction of the $A'[A_{n-1}Nb_nO_{3n+1}]$ Dion−Jacobson phases with $n = 3$ could lead to metallic conductivity, in contrast with the results for the $n = 2$ phases.

Introduction

The study of layered perovskite oxides with transition metals other than copper is of great interest for the possible implications of this kind of system on superconductivity. In this respect, a very recent report of superconductivity in the oxide Sr_2RuO_4[2] has reawakened the controversy of the unique role of copper in high T_c superconductivity and has introduced a new key element in the theoretical discussion of this phenomenon.[3] Several examples of superconducting transition metal oxides can be found in the literature earlier than 1987. Among them there are various phases containing early transition metals and presenting a number of different structures.[4] Yet Sr_2RuO_4 represents the first example of a copperless superconductor with the typical topology of corner-sharing octahedra found in high T_c superconductors. It presents though a different electron count, spin state, and an added novelty: no doping is necessary to attain superconductivity.

Our interest in this field of solid state chemistry has led us to work on the preparation, characterization and doping of a series of layered oxides of niobium with general formula $ALaNb_2O_7$, where A denotes H, alkali metal, or Ag atoms. These oxides present a layered structure formed by double perovskite slabs of La−Nb−O with A^+ ions intercalated between them. The alkali ions are easily interchanged leading to interesting ion-exchange properties.[5−7] We have recently shown the possibility of doping these oxides by intercalation of additional ions at room temperature or by high temperature reduction methods.[8] Due to the doping, the niobium atoms of these materials are in a $Nb^{(5-x)+}$ oxidation state. This may lead one to expect these materials to be metallic. However, they exhibit a thermally activated conduction. $Sr_3V_2O_7$, the second member of the $Sr_{n+1}V_nO_{3n+1}$ series of layered oxides, is also made up of double perovskite slabs and is a metal down to low temperatures.[9] However, the vanadium atoms in $Sr_3V_2O_7$ are in a lower oxidation state, V^{4+}. Thus it seems that the filling of the bands of these double octahedral slabs can be an important parameter to control in order to prepare new metallic (or maybe superconducting) oxides with this structure.

Another important parameter to control is the internal structure of the double layers. Recent work in molybdenum and tungsten oxides and bronzes has shown how important slight distortions of the MO_6 octahedra can be in controlling the transport properties of these low-dimensional systems.[10] Quite recently, Armstrong and Anderson[11] have reported the synthesis and structure of a new phase built from double perovskite slabs, $Rb_2LaNb_2O_7$. Whereas the octahedra in $Sr_3V_2O_7$ are quite regular, the two axial Nb−O distances are noticeably different in $Rb_2LaNb_2O_7$. It is not clear how the electronic structure and transport properties of the double octahedral slabs will be affected by such a distortion. In addition, the oxidation state of the niobium atoms in $Rb_2LaNb_2O_7$ (i.e., $Nb^{4.5+}$) is different from that of the vanadium atoms in $Sr_3V_2O_7$ (V^{4+}). Interestingly, it has also been suggested that $Sr_3V_2O_7$ is still another example of a metal exhibiting the so-called hidden Fermi surface nesting.[12] All these facts prompted us to examine in some detail

[⊗] Abstract published in *Advance ACS Abstracts,* January 15, 1996.

(1) (a) Permanent address: Department of Chemistry, The University of Michigan, Ann Arbor, Michigan 48109. (b) Permanent address: Laboratoire de Chimie Théorique (URA CNRS 506), Université de Paris Sud, 91405 Orsay Cédex, France.
(2) Maeno, Y.; Hashimoto, H.; Yoshida, K.; Nishizaki, S.; Fujita, T.; Bednorz, J. G.; Lichtenberg, F. *Nature* **1994**, *372*, 532.
(3) Fisk, Z. *Nature* **1994**, *372*, 502.
(4) See for instance: Tsuda, N.; Nasu, K.; Yanase, A.; Siratori, K. *Electronic Conduction in Oxides*; Springer-Verlag: Berlin, 1991.
(5) (a) Dion, M.; Ganne, M.; Tournoux, M. *Mater. Res. Bull.* **1981**, *16*, 1429. (b) Dion, M.; Ganne, M.; Tournoux, M. *Rev. Chim. Miner.* **1986**, *23*, 61.
(6) (a) Jacobson, A. J.; Lewandowski, J. T.; Johnson, J. W. *J. Less-Common Met.* **1986**, *116*, 137. (b) Jacobson, A. J.; Johnson, J. W.; Lewandowski, J. T. *Inorg. Chem.* **1985**, *24*, 3727. (c) Jacobson, A. J.; Johnson, J. W.; Lewandowski, J. T. *Mater. Res. Bull.* **1987**, *22*, 45.
(7) (a) Gopalakrishnan, J.; Bhat, V.; Raveau, B. *Mater. Res. Bull.* **1987**, *22*, 413. (b) Sato, M.; Abo, J.; Jin, T.; Ohta, M. *Solid State Ionics* **1992**, *51* , 85. (c) Sato, M.; Abo, J.; Jin, T. *Solid State Ionics* **1992**, *57*, 285. (d) Sato, M.; Watanabe, J.; Uematsu, K. *J. Solid State Chem.* **1993**, *107*, 460.
(8) (a) Gómez-Romero, P.; Palacín, M. R.; Casañ-Pastor, N.; Fuertes, A. *Solid State Ionics* **1993**, *63*−65, 424. (b) Palacín, M. R.; Lira, M.; García, J. L.; Caldés, M. T.; Casañ-Pastor, N.; Fuertes, A.; Gómez-Romero, P. *Mater. Res. Bull.*, in press.
(9) (a) Nozaki, A.; Yoshikawa, H.; Wada, T.; Yamauchi, H.; Tanaka, S. *Phys. Rev. B* **1991**, *43*, 181. (b) Suzuki, N.; Noritake, T.; Yamamoto, N.; Hiroki, T. *Mater. Res. Bull.* **1991**, *26*, 1.
(10) (a) Canadell, E.; Whangbo, M.-H. *Chem. Rev.* **1991**, *91*, 965. (b) Whangbo, M.-H.; Canadell, E. *Acc. Chem. Res.* **1989**, *22*, 375.
(11) Armstrong, A. R.; Anderson, P. A. *Inorg. Chem.* **1994**, *33*, 4366.
(12) Whangbo, M.-H.; Ren, J.; Liang, W.; Canadell, E.; Pouget, J.-P.; Ravy, S.; Williams, J. M.; Beno, M. A. *Inorg. Chem.* **1992**, *31*, 4169.

0020-1669/96/1335-1179$12.00/0

the electronic structure of oxides containing double perovskite layers in order to have some hint as to how the electron filling and structural distortions can be related to their transport properties. Our calculations are of the extended Hückel tight binding type[13] which have been very successful in correlating the structural and transport properties of many low-dimensional transition metal oxides and bronzes.[10,14]

Crystal Structure

As shown in **1**, a MO_4 layer can be formed from MO_6 octahedra by sharing the four equatorial oxygen atoms (O_{eq}).

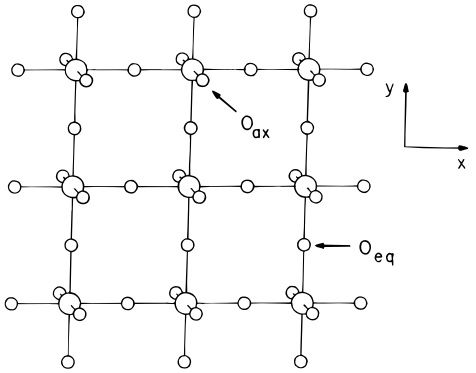

1

Then, a M_2O_7 double layer (**2**) can be formed from two MO_4

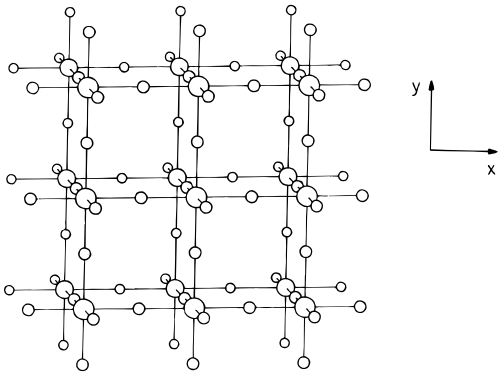

2

layers by sharing their axial oxygen atoms (O_{ax}). Filling the center of every cubic hole in **2** with an A cation leads to the AM_2O_7 layer which is a fragment of the perovskite structure. It is the stacking of these double perovskite slabs interweaved by further cations which leads to the crystal structure of $Rb_2LaNb_2O_7$,[11] $Sr_3V_2O_7$,[9] and $A'LaNb_2O_7$ ($A' = H$, alkali metal, or Ag atoms).[5−8] The relative position of these double perovskite slabs can change from one compound to the other. However this is not relevant in the context of the present work because the transport properties of these systems should be mainly controlled (but see later) by the electronic structure of the $M_2O_7^{n-}$ double octahedral slabs. Important for our discussion will be the internal structure of these slabs. In $Sr_3V_2O_7$ the two outer $M-O_{ax}$ bonds are shorter than the two inner ones, although the $M-O$ bond lengths are quite uniform ($M-O_{ax}$ = 1.97, 1.87 Å; $M-O_{eq}$ = 1.92 Å) and the $M-O_{ax}-M$ angle is 180°. In contrast, the difference between the two $M-O_{ax}$ bonds in $Rb_2LaNb_2O_7$ is clearly larger ($M-O_{ax}$ = 2.111, 1.842 Å; $M-O_{eq}$ = 2.029, 2.053 Å) and the $M-O_{ax}-M$ angle is 163.8°. Thus, the double octahedral layers of $Sr_3V_2O_7$ are not far from what could be considered an "ideal" layer but those of $Rb_2LaNb_2O_7$ are considerably distorted. Also of interest for our subsequent discussion is that the departure from the "ideallity" seems to be even larger in the parent compound $RbLaNb_2O_7$ where the niobium atoms are in a Nb^{5+} oxidation state ($M-O_{ax}$ = 2.277, 1.774 Å; $M-O_{eq}$ = 1.949, 2.024 Å; $M-O_{ax}-M$ = 165.3°).

Electronic Structure

Assuming the oxidation states O^{2-}, La^{3+}, Sr^{2+} and A'^{+} (A' = H, alkali metal or Ag atoms), the transition metal atoms in the M_2O_7 layers of the phases mentioned before have electron counts between d^0 and d^1. Thus, to understand how their crystal structures and transport properties are correlated, we need to understand how the octahedral distortions control the nature of the bottom part of the t_{2g}-block bands. In order to make the analysis applicable to any M_2O_7 layer, let us first consider an ideal double octahedral layer (with all $M-O$ distances identical and all angles equal to 90° and 180°) and later see how the departure from ideallity can modify the results.

A. Ideal M_2O_7 Layer. As shown elsewhere,[10] for many transition metal oxides and bronzes with low d-electron counts, the bottom part of the t_{2g}-block bands can be understood in an extremely simple way. The d-block band levels of a crystal structure obtained by sharing octahedral corners are raised in energy when the orbitals of the bridging oxygen atoms are allowed by symmetry to mix with the metal d orbitals. Thus, all that should be done to evaluate the dispersion of the bands is just count how many oxygen p orbital contributions can be found in the crystal orbitals for different points of the Brillouin zone. In the present case a similar procedure can be used. Let us start with the single octahedral layer shown in **1**. The crystal orbitals for the xy orbital at Γ, X, and M are shown in **3a**−**c**

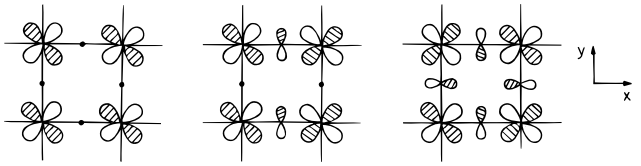

3a **3b** **3c**

where dots indicate the absence of oxygen p orbitals. Those for the *xz* and *yz* orbitals are shown in **4a**−**c** and **5a**−**c**,

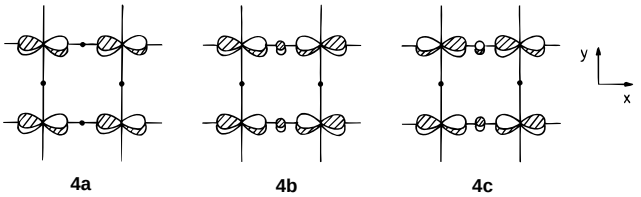

4a **4b** **4c**

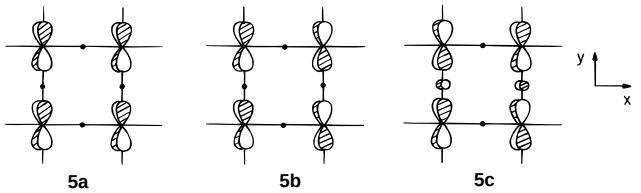

5a **5b** **5c**

(13) Whangbo, M.-H.; Hoffmann, R. *J. Am. Chem. Soc*. **1978**, *100*, 6093. A modified Wolfsberg−Helmholz formula (Ammeter, J. H.; Bürgi, H.-B.; Thibeault, J.; Hoffmann, R. *J. Am. Chem. Soc*. **1978**, 100, 3686) was used to evaluate the off-diagonal $H_{\mu\nu}$ values. The atomic parameters used in the calculations were taken from previous work (Canadell, E.; Jobic, S.; Brec, R.; Rouxel, J.; Whangbo, M.-H. *J. Solid State Chem*. **1992,** *99*, 189; Whangbo, M.-H.; Schneemeyer, L. F. *Inorg. Chem*. **1986**, *25*, 2425).

(14) Canadell, E.; Whangbo, M.-H. *Phys. Rev. B* **1991**, *43*, 1894 (1991).

Table 1. Antibonding Contributions per Unit Cell of the Oxygen p Orbitals in the t_{2g}-Block Bands of the MO_4 Octahedral Lattice **1**

band	crystal orbital	wave vector point	bridging contributions	axial contributions
xy	**3a**	Γ	NN	nn
	3b	X	YN	nn
	3c	M	YY	nn
xz	**4a**	Γ	NN	yy
	4b	X	YN	yy
	4c	M	YN	yy
yz	**5a**	Γ	NN	yy
	5b	X	NN	yy
	5c	M	NY	yy

respectively. In the present case, a qualitative band diagram can only be obtained if the oxygen contributions from the axial oxygen atoms (O_{ax}, see **1**) are also taken into account. For simplicity, these axial contributions are not shown in **3**−**5**. However, it is obvious that there are two axial contributions per metal atom in **4a**−**c** and **5a**−**c** but none in **3a**−**c**. The total number of oxygen antibonding contributions per unit cell to the *xy*, *xz*, and *yz* crystal orbitals are summarized in Table 1, where Y/N and y/n indicate the presence/absence of such contributions in the bridging and axial oxygen positions, respectively. As shown elsewhere,[10] the energy destabilization of an oxygen p contribution in the bridging (Y) and axial (y) positions are related through the relationship Y ≈ 4y. Thus, a qualitative band structure for the MO_4 single octahedral layer can be obtained (**6**) by counting the total number of oxygen

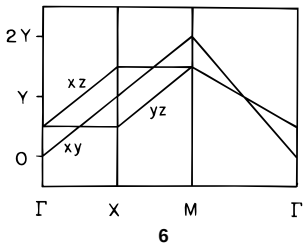

6

contributions and using that relation.

Construction of a qualitative band structure for the M_2O_7 double octahedral layer is now simple. The orbitals of each M−O_{ax}−M linkage leading to the six t_{2g}-block bands are shown in **7a**−**b**, **8a**−**b**, and **9a**−**b** (for simplicity, the contributions of

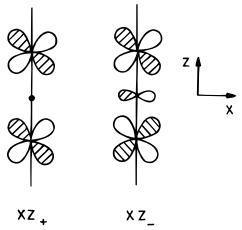

7a **7b**

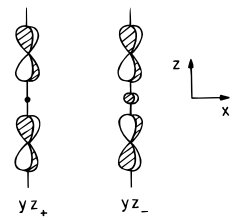

8a **8b**

the nonbridging O_{ax} orbitals are not shown in **7**−**9**). The xy_+ (**9a**) and xy_- (**9b**) combinations are practically degenerate because the bridging p orbitals of the O_{ax} atom cannot interact with the *xy* orbitals due to the δ symmetry along the M−O_{ax}−M

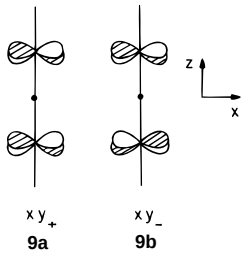

9a **9b**

axis. The number of oxygen p orbital contributions per unit cell of the double octahedral layer to the xy_+ and xy_- bands are thus identical and just twice those of the single octahedral layer. The xz_+ (**7a**) and yz_+ (**8a**) combinations are lower than the xz_- (**7b**) and yz_- (**8b**) because they do not have p orbital contributions at the bridging axial position. The number of oxygen p orbital contributions per unit cell of the double octahedral layer to the xz_+ and yz_+ bands are twice those of the single octahedral layer minus two axial contributions (2y = Y/2). Those of the xz_- and yz_- bands are the same as those of the xz_+ and yz_+ bands plus one bridging contribution (Y) coming from the M−O_{ax}−M position. Thus the qualitative band structure for the double octahedral layer can be easily constructed and is shown in **10**.

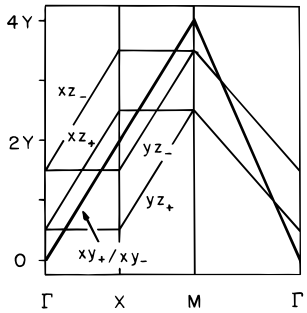

10

B. Real M_2O_7 Layers. It is clear from **10** that although the bottom of the xy_+/xy_- bands is the lowest part of the t_{2g}-block bands, the xz_+ and yz_+ bands overlap with the xy_+/xy_- ones for most electron counts. Although it depends on the actual strength of the M−O interaction, model calculations show that the Fermi level should lie at the band crossing when the electron count at the metal atom is around $d^{1/4}$. As shown in **10**, whereas the xz_+ and yz_+ bands are one dimensional (1D), the xy_+ and xy_- are two dimensional (2D). Thus, for most metal electron counts the Fermi surface of the layer will result from the hybridization of two open 1D Fermi surfaces originating from the xz_+ and yz_+ bands and two closed 2D Fermi surfaces originating from the xy_+ and xy_- bands. Because of the local orthogonality of the three t_{2g} orbitals, the hybridization will be very weak and the total Fermi surface will practically result from the superposition of these four Fermi surfaces. Thus, in principle these systems could exhibit low temperature Fermi surface instabilities, like charge density wave (CDW) or spin density wave (SDW), which could destroy the 1D portions of the Fermi surface. However, if the xz_+/yz_+ bands are raised as a result of some structural distortion, the Fermi level for metal electron counts between d^0 and d^1 could cross the xy_+/xy_- bands only, and thus, the Fermi surface of the layer would then be the superposition of two closed 2D Fermi surfaces. In such case the system would be immune to CDW or SDW instabilities.

According to our analysis of the ideal M_2O_7 double layer, the difference between the bottom of the xy_+/xy_- and xz_+/yz_+ bands is given by the two p orbital contributions of the non bridging O_{ax} atoms (i.e., 2y = Y/2). Thus, the xz_+/yz_+ bands

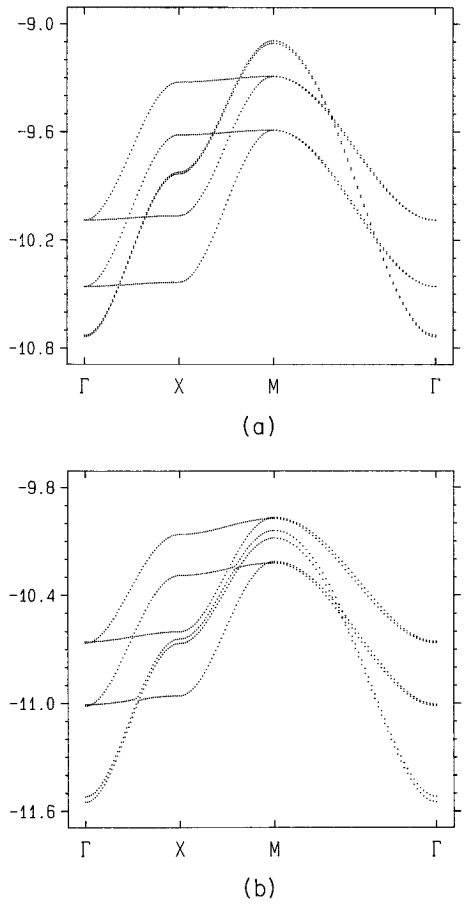

Figure 1. Dispersion relations for the t_{2g}-block bands calculated for the M_2O_7 double octahedral slabs of (a) $Sr_3V_2O_7$ and (b) $Rb_2LaNb_2O_7$ assuming an Nb−O_{ax}−Nb angle of 180°. Γ, X, and M refer to the wave vectors (0, 0), (**a***/2, 0), and (**a***/2, **a***/2), where **a** is the repeat vector of the square lattice.

will be raised up in energy if the nonbridging M−O_{ax} distances are shorter that the mean M−O distance, which in general will coincide with the M−O_{eq} distance. As mentioned before, the octahedra are quite regular in $Sr_3V_2O_7$ but noticeably distorted in $Rb_2LaNb_2O_7$. Thus, whereas the nonbridging M−O_{ax} bond length in $Sr_3V_2O_7$ is only 0.048 Å shorter than the average M−O distance, the difference is almost four times larger (0.178 Å) in $Rb_2LaNb_2O_7$. Consequently, it is expected that the xz_+/yz_+ band will lie considerably higher in energy in the second case. The calculated band structures for the M_2O_7 slabs of $Sr_3V_2O_7$ and $Rb_2LaNb_2O_7$ (assuming in this case an Nb−O_{ax}−Nb angle of 180°) are shown in Figure 1, respectively. The general shape of these band structures is in excellent agreement with the model band structure **10**. The total width of the xy_+/xy_- bands is practically the same in both calculations. The important difference is that the xz_+/yz_+ bands are shifted to higher energies in Figure 1b. Thus, the bottom of the xy_+/xy_- and xz_+/yz_+ bands are separated by 0.27 eV in Figure 1a but by 0.53 eV in Figure 1b. It is also worthy of mention that the energy difference between the xz_+/yz_+ and the xz_-/yz_- bands is not very different in parts a and b of Figure 1 (0.35 vs 0.32 eV, respectively). This is because this energy difference is given by the p orbital contribution of the bridging O_{ax} atom (i.e., Y). This energy difference will thus decrease as the difference between the inner M−O_{ax} bond length and the M−O_{eq} (or the average M−O) distance will increase. These bond length differences (Å) are now not so different: 0.052 (0.053) for $Sr_3V_2O_7$ and 0.071 (0.091) for $Rb_2LaNb_2O_7$. Most of the details of these band structures can be easily explained in a similar vein. The important result however is the largest energy difference between the bottom of the xz_+/yz_+ and xy_+/xy_- bands in Figure 1b.

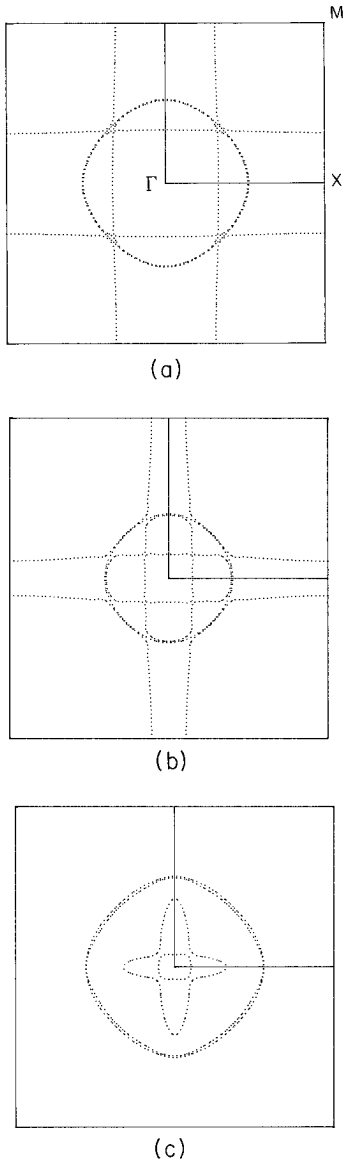

Figure 2. Fermi surfaces calculated for the V_2O_7 double octahedral slabs of $Sr_3V_2O_7$ with metal electron counts of d^1 (a) and $d^{0.5}$ (b) and for the Nb_2O_7 double octahedral slabs of $Rb_2LaNb_2O_7$ ($d^{0.5}$) assuming an Nb−O_{ax}−Nb angle of 180° (c).

The Fermi levels calculated assuming $d^{0.5}$ and d^1 metal electron counts for the V_2O_7 lattice of $Sr_3V_2O_7$ cut both the xy_+/xy_- and xz_+/yz_+ bands. Thus, the total Fermi surfaces for both d^1 (Figure 2a) and $d^{0.5}$ (Figure 2b) contain two closed 2D portions (originating from the xy_+/xy_- bands) and two open 1D portions along perpendicular directions (originating from the xz_+/yz_+ bands). The situation is different for the Nb_2O_7 lattice of Figure 1b. Whereas for a d^1 metal electron count the Fermi surface is very similar to that of Figure 2a, for $d^{0.5}$ the Fermi level cuts just the bottom of the xz_+/yz_+ bands so that the Fermi surface contains essentially two practically superposed and almost circular closed portions (see Figure 2c). However there are also remnants of the two 1D portions at the center of the Brillouin zone, although they are closed and small. Thus, the bond alternation perpendicular to the slab changes the nature of the Fermi surface for metal electron counts around $d^{0.5}$ but does not qualitatively change that for metal electron counts around d^1.

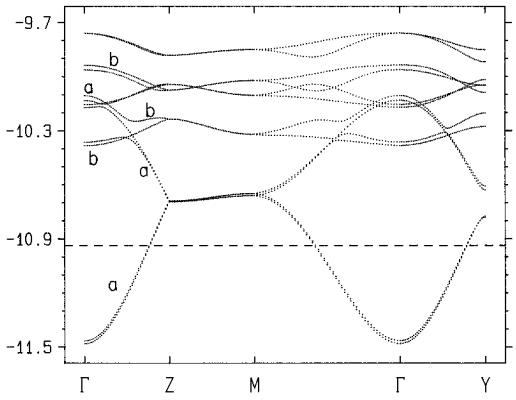

Figure 3. Dispersion relations for the t_{2g}-block bands of the Nb_2O_7 double octahedral slabs of $Rb_2LaNb_2O_7$ using the experimental structure. The dashed line refers to the Fermi level ($d^{0.5}$). Γ, Y, Z, and M are the wave vectors (0, 0), (**b***/2, 0), (0, **c***/2,), and (**b***/2, **c***/2), respectively.

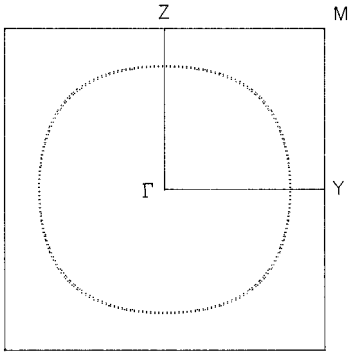

Figure 4. Fermi surfaces calculated for the $Nb_2O_7^{5-}$ double octahedral slabs of $Rb_2LaNb_2O_7$ using the experimental structure.

At this point it should be noted that since the Nb−O−Nb angle is different from 180°, the unit cell of the double octahedral layer in $Rb_2LaNb_2O_7$ is twice as large and the unit cell axis are rotated by 45° with respect to those used for the calculations of Figure 1b. Thus the area of the unit cell in reciprocal space is half that of the same lattice when the Nb−O−Nb angle is 180°. Consequently, every pair of bands along Γ → M of Figure 1b should appear as a pair of almost doubly folded bands along the Γ → Y and Γ → Z directions in the band structure of the real lattice shown in Figure 3 (Note that the double octahedral slabs in the experimental structure are parallel to the (*bc*) plane of the orthorhombic unit cell. For clarity, however, we keep the same notation for the orbitals). Two points of Figure 3 are worth noting. First, the energy difference between the bottom of the xy_+/xy_- and xz_+/yz_+ bands (denoted a and b, respectively, in Figure 3) has increased. Thus, the Fermi level is now well below the xz_+/yz_+ bands and the Fermi surface (see Figure 4) just contains the two closed almost superimposed portions due to the xy_+/xy_- bands.[15] Assuming a rigid band scheme, the shape of the Fermi surface would be retained up to metal electron counts around $d^{0.75}$. Second, the xz_+/yz_+ and xz_-/yz_- bands are quite flat in contrast with the same bands in Figure 1b. This is not the case however for the xy_+/xy_- bands. These two observations are obviously related to the structural deformations of the double octahedral layer in $Rb_2LaNb_2O_7$ which are of two types. First, a bending of the Nb−O_{ax}−Nb angle (∼165°). Second, an off-plane distortion of the O_{eq} atoms in such a way that two of the O_{ax}−Nb−O_{eq} angles are 94° and two are 100°. Model calculations for corner sharing double octahedra show that bending of the Nb−O_{ax}−Nb angle up to the experimental value has practically no effect on the six t_{2g} levels. In contrast, the off-plane distortion of the equatorial oxygen atoms raises noticeably the xz_+/yz_+ levels and consequently, leads to the larger gap between the bottom of the xy_+/xy_- and xz_+/yz_+ bands in the band structure of Figure 3. The xz_+/yz_+ levels raise up[16] because the off-plane distortion of the O_{eq} atoms allows the mixing of the basal ligand orbitals in a σ antibonding way. As a result, the metal xz/yz orbitals hybridize away from the O_{eq} and toward the nonbridging O_{ax} atom (see **11** where the basal O_{eq} orbitals are not shown for clarity). This hybridization reduces the antibonding Nb−O_{eq} σ^* interaction at the expense of an increased antibonding π^* interaction with the nonbridging O_{ax} atom which, we note, is associated with a quite short Nb−O distance. Obviously, the off-plane distortion of the O_{eq} atoms is also at the origin of the decrease of the dispersion of the xz_+/yz_+ and xz_-/yz_- bands in Figure 3, because both the distortion and the hybridization decrease the π type interaction between adjacent *xz*/*yz* metal orbitals through the equatorial oxygen orbitals. This off-plane distortion does slightly stabilize the xy_+/xy_- levels because it decreases the M(*xy*)−O(p) π type overlap but the effect is small so that the total dispersion of the xy_+/xy_- bands is almost left unaltered. These results clearly show that both bond alternations perpendicular to the layer and off-plane distortion of the O_{eq} atoms have a strong influence on the Fermi surface of double octahedral slabs when the metal d electron count is lower than d^1.

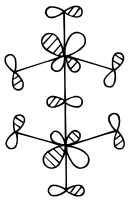

11

C. Electronic Structure and Transport Properties. Let us now try to correlate the previous results with the transport properties of these materials. As mentioned, $Sr_3V_2O_7$ is metallic[9] but no conductivity measurements have been reported for $Rb_2LaNb_2O_7$. Although the Fermi surfaces of the two phases are different, the dispersion of the partially filled bands are very similar and large. This result and the fact that there is only one type of niobium atom in the structure suggest that $Rb_2LaNb_2O_7$ should also be metallic. According to the calculated Fermi surface of Figure 4, it should be a 2D metal with very isotropic conductivity within the (*bc*) plane and should retain its metallic properties down to low temperatures. If it is possible to carry out magnetoresistance experiments, the system could show one Shubnikov−de Haas frequency corresponding to an area of half the Brillouin zone. Our study suggests however that this should not be generalized to other double octahedral layers with $d^{0.5}$ metal electron counts. Depending on the M−O bond alternation perpendicular to the layer and the puckering of the O_{eq} atoms, the Fermi surface will also contain two perpendicular 1D portions in addition to the 2D ones. In such case, although the hybridization between the 1D and 2D parts is weak, there are several closed loops in the surface. Consequently, several Shubnikov−de Haas frequencies will be found in the magnetoresistance experiments. More

(15) Note that the area of the Fermi surface of Figure 4 looks twice as large as that of Figure 2c. This is due to the fact that the area of the unit cell in reciprocal space has been reduced by half because of the unit cell doubling in real space.

(16) Wheeler, R. A.; Whangbo, M.-H.; Hughbanks, T. R.; Hoffmann, R.; Burdett, J. K.; Albright, T. A. *J. Am. Chem. Soc*. **1986**, *108*, 2222.

importantly, the two 1D portions are well nested so that the system could then exhibit low temperature resistivity anomalies associated with CDW or SDW anomalies. However, these anomalies would only destroy the 1D portions of the Fermi surface so that the system is expected to keep its metallic properties after the transition. The last scenario is most likely to apply for any d^1 system whatever it is the structure of the double perovskite slab.

As mentioned before, n-doping of $HLaNb_2O_7$ at 650° transforms the white insulator precursor into a blue solid with semiconducting properties.[8b] The poor crystallinity of the samples prevented the study of the structural changes brought about by the reduction. However, whether the structure is tetragonal (as suggested for undoped d^0 $HLaNb_2O_7$[7]) or orthorhombic (as for $d^{0.5}$ $Rb_2LaNb_2O_7$[11]), the band structures of Figures 1b and 3 suggest that the dispersion of the xy_+/xy_- bands (most likely the only partially filled ones) is again large and comparable to that of metallic $Sr_3V_2O_7$. Thus, poor crystallinity and oxygen vacancies can be considered to be at the origin of the semiconducting properties. However, we believe that even if better samples could be obtained they still would be semiconducting. The low density of carriers in the system, as well as the existence of disorder both in between the layers (due to the doping atoms) and within the layers (due to the oxygen vacancies), makes these phases ideally suited to exhibit some type of Anderson localization. This does not mean that metallic phases can not be obtained by chemical reduction of the so called Dion−Jacobson phases $A'[A_{n-1}Nb_nO_{3n+1}]$.[5−7,11] Two possible strategies to approach the problem can be considered: first, doping of the double layer oxide at low temperatures to avoid the formation of vacancies and disorder; second, screening of the conducting electrons from the random potentials in the interlayer region. This can be realized by using the next member of the series ($n = 3$), which contains triple perovskite slabs, provided that the outer octahedra of the layer are strongly distorted whereas those of the inner sublayer are quite regular. Under such conditions, the lowest part of the t_{2g}-block bands will be an *xy* type band almost completely localized in the inner octahedral sublayer of the triple perovskite slab.[10] In addition, in this case the conducting electrons will not be shared by two bands, as in the $n = 2$ phases, so that the density of carriers can be relatively high. As a matter of fact, the crystal structure of the $n = 3$ phase $CsCa_2Nb_3O_{10}$[17] exhibits exactly the type of distortions needed. We thus suggest that chemical reduction experiments of the $n = 3$ phases would be very interesting. For $n > 3$ the density of carriers will start to decrease again so that even if the system would be screened from the interlayer random potentials, the low density of carriers will provide small screening from local imperfections or small distortions and the reduced phases could be again localized.

(17) Dion, M.; Ganne, M.; Tournoux, M.; Ravez, J. *Rev. Chim. Miner.* **1984**, *21*, 92.

Concluding Remarks

The electronic structure of phases containing double octahedral M_2O_7 layers with low d electron counts is strongly dependent of the d electron count and the distortions of the layer. All d^1 systems are expected to be similar and to have Fermi surfaces which result from the superimposition of both 1D and 2D contributions. For lower d electron counts, the electronic structure is quite sensitive to the existence of M−O bond alternation perpendicular to the layer and off-plane distortions of the O_{eq} atoms. The Fermi surfaces can either be purely 2D or have 1D and 2D portions, like those of the d^1 systems. The recently reported phase $Rb_2LaNb_2O_7$ could be a 2D metal with a closed Fermi surface and thus with no possibility of low temperature structural instability. The d^1 systems could exhibit metal to metal transitions associated with the 1D portions of their Fermi surface. Our study also suggests that chemical reduction of the $A'[A_{n-1}Nb_nO_{3n+1}]$ phases with $n = 3$ could lead to metallic conductivity. Finally, let us note that although there is an obvious structural relationship of these layered systems with high T_c superconductors, our study makes clear that from the electronic viewpoint the situation is very different.[18,19]

Acknowledgment. This work has been funded by the DGICYT (Spain) (Project PB93-0122). R.R. would like to thank the NSERC of Canada for a postgraduate research fellowship and M.R.P. the Generalitat de Catalunya for a predoctoral fellowship. E. C. would like to thank the CNRS for a sabbatical which made the stay at ICMAB possible.

IC951048U

(18) For a related study concerning this point, see: Albright, T. A.; Yee, K. A.; Whangbo, M.- H.; Jung, D. *Angew. Chem., Int. Ed. Engl.* **1989**, *28*, 750.

(19) After completion of this work we became aware of the existence of a resistivity anomaly attributed to a CDW instability in the $Ln_3Ni_2O_7$ phases, which also contain $M_2O_7^{n-}$ double octahedral slabs (Seo, D. K.; Whangbo, M.-H.; Zhang, Z.; Greenblatt, M., to be submitted for publication). The partially filled bands of these phases are, however, the e_g-block bands. The CDW instability in this material has also been attributed to hidden 1D Fermi surface nesting, which seems to depend very sensitively on the octahedral distortions of the double layer. We thank the authors for communication of these results before publication.